# Generalized Joint Channel–Network Coding in Asymmetric Two-Way Relay Channels

**Shengqiang Shen[1], Shiyin Li [1] and Zongyan Li [1]**
[1] School of Information and Control Engineering, China University of Mining and Technology
Xuzhou, Jiangsu 221000 - China
[e-mail: jhnsnshen@cumt.edu.cn, lishiyin@cumt.edu.cn, lizongyan@cumt.edu.cn]
*Corresponding author: Shiyin Li

*Received October 18, 2015; revised April 18, 2016; accepted November 15, 2016; published December 31, 2016*

## Abstract

Combining channel coding and network coding in a physical layer in a fading channel, generalized joint channel–network coding (G-JCNC) is proved to highly perform in a two-way relay channel (TWRC). However, most relevant discussions are restricted to symmetric networks. This paper investigates the G-JCNC protocols in an asymmetric TWRC (A-TWRC). A newly designed encoder used by source nodes that is dedicated to correlate codewords with different orders is presented. Moreover, the capability of a simple common non-binary decoder at a relay node is verified. The effects of a power match under various numbers of iteration and code lengths are also analyzed. The simulation results give the optimum power match ratio and demonstrate that the designed scheme based on G-JCNC in an A-TWRC has excellent bit error rate performance under an appropriate power match ratio.

***Keywords:*** Asymmetric two-way relay, G-JCNC, virtual encoder, power matching, iteration numbers

This work was supported by The Key Technologies R & D Program of Jiangsu Province, China (Grant No.SBE2014001019); The Emergency Management Program of the National Natural Science Foundation of China (Grant No.51541410).

**http://dx.doi.org/10.3837/tiis.2016.12.013** **ISSN : 1976-7277**

## 1. Introduction

In recent years, network coding (NC) and cooperative relaying have been widely studied [1][2][3] to improve network performance. A two-way relay channel (TWRC) is one of the typical scenarios that can be applied by NC to enhance throughput. In a TWRC system, the relay node acts as a conveyor for the two source nodes. The relay may adopt a physical-layer network coding (PLNC) [4][5][6] protocol to complete whole communications within two phases. As the original PLNC neglects the effect of channel coding [6][7], joint channel–network coding (JCNC) was proposed in [6][7] in an attempt to merge channel coding with NC. Several schemes based on different channel coding, such as repeat–accumulate (RA) codes in [8] and low-density parity-check (LDPC) codes in [9][10], have been studied. As these schemes are based on additive white Gaussian noise channels with binary phase-shift keying (BPSK) modulation, a generalisation of JCNC that considers fading channels called generalized JCNC (G-JCNC) with BPSK modulation was presented in [11] and that with quadtrature phase-shift keying (QPSK) modulation was discussed in [12]. These aforementioned works are restricted to the assumption that the channels between two source nodes and relay node are symmetric. However, the qualities of the channels in TWRC are practically always asymmetric [13]. Therefore, asymmetric modulations should be considered to achieve asymmetric transmission. The authors of [14] pointed out that the symbol error rate in the multiple access phase is affected by the power matching ratio of the two source nodes in TWRC. The performance of the original PLNC in an asymmetric TWRC (A-TWRC) was examined in [15][16][17][18][19] when the two source nodes employ asymmetric modulations. To the best of our knowledge, no other paper or study has examined the G-JCNC scheme in an A-TWRC scenario.

In a symmetric situation, two source nodes adopt the same linear code without extra modifications. Therefore, the decoder at the relay node simply selects the tanner graph corresponding to the encoders at the source nodes. Special belief propagation is also required. However, modifications should be introduced into the source nodes in an asymmetric situation. In this paper, the multiple-access phase of an A-TWRC is designed based on the G-JCNC.

First, an encoding approach is designed to correlate codewords from the source nodes to make a common non-binary linear decoder suitable for decoding at the relay node.

Second, the capability of the non-binary decoder at the relay node is verified by proving that the superposition of the codewords from the source nodes is only the output of a virtual encoder, which inputs the superposition of the corresponding uncoded messages.

Finally, the optimum power matches under the effects of several different parameters, including iteration number and code length, which are rarely mentioned in other papers, are discussed.

The rest of this paper is organised as follows. Section II introduces the model of a two-way relaying system. A brief procedure of a common symmetric situation from the literature [11][12] is reviewed. In Section III, the designed scheme based on the G-JCNC in the A-TWRC scenario is provided from the encoder at the source nodes and the decoder at the relay node to the decoder at source nodes in an order of data flow. In Section IV, we analyze the effect of power matching of the paired transmitters on the different parameters. The performances of the designed scheme under different signal to noise ratios (SNRs) are compared. Section V concludes.

## 2. System Model

The TWRC system with two source nodes, A and B, and one relay node, R, is illustrated in **Fig. 1**. As A and B have no direct links between them, they need to exchange information through the relay node R. All nodes are assumed to operate in a half-duplex mode and to be perfectly synchronized.

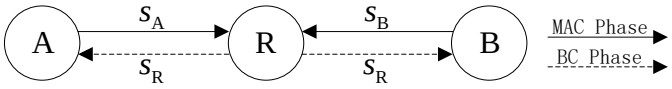


**Fig. 1.** TWRC model with two phases

Let $\mathbf{u}_A$ and $\mathbf{u}_B$ denote the uncoded words of length $K$ of source nodes A and B, respectively. These words are encoded by the same linear channel code $\Gamma$ into the codewords $\mathbf{c}_A = \Gamma(\mathbf{u}_A)$ and $\mathbf{c}_B = \Gamma(\mathbf{u}_B)$ of length $N$. Subsequently, the codewords are modulated by the same order modulator to $\mathbf{s}_A = \mathcal{M}\{\mathbf{c}_A\}$ and $\mathbf{s}_B = \mathcal{M}\{\mathbf{c}_B\}$.

The two-way relay exchange comprises a multiple access (MA) phase in time slot 1 and a broadcast (BC) phase in time slot 2. In the MA phase, both source nodes transmit $\mathbf{s}_A$ and $\mathbf{s}_B$ to the relay node R simultaneously. Therefore, the received signal at the relay node R is:

$$\mathbf{y}_R = \mathbf{h}'_A \mathbf{s}_A + \mathbf{h}'_B \mathbf{s}_B + \mathbf{n}_R \tag{1}$$

where $\mathbf{y}_R$ is the linear superposition of the transmit signals, and $\mathbf{h}'_A$ and $\mathbf{h}'_B$ are the fading channel coefficients. $\mathbf{n}_R$ denotes the noise vector at the relay node R, the elements of which are i.i.d zero-mean complex Gaussian random variables with variance of $\sigma_n^2$.

Perfect channel state information (CSI) is assumed to be available at all the nodes. As mentioned in [20], phase deviation can contribute in improving performance. Therefore, the source nodes can eliminate the amplitude deviations while using phase deviations by multiplying the symbol $s_A$ by $1/|h'_A|$ and the symbol $s_B$ by $1/|h'_B|$. Thus we have:

$$y_R = \frac{h'_A}{|h'_A|} s_A + \frac{h'_B}{|h'_B|} s_B + n_R = h_A s_A + h_B s_B + n_R \tag{2}$$

where $h_A$ and $h_B$ are the normalized fading channel coefficients. The effect of the imperfect channel estimation on the system performance is also evaluated in Section IV.

Then XOR, which is a commonly used NC, of the source codewords $\mathbf{c}_{A\oplus B} = \mathbf{c}_A \oplus \mathbf{c}_B$ is estimated from $\mathbf{y}_R$ at the relay node R. Afterwards, the relay node R modulates the estimated relay codeword $\mathbf{c}_R = \mathbf{c}_{A\oplus B}$ to $\mathbf{s}_R = \mathcal{M}\{\mathbf{c}_R\}$ and broadcasts it to both source nodes A and B simultaneously in the BC phase. Thus, the signals received at source nodes A and B are given by $y_A = h'_A s_R + n_A$ and $y_B = h'_B s_R + n_B$. Then, source node A can estimate the information $\mathbf{u}_{R,A}$ from $\mathbf{y}_A$ and obtain the information sent by source node B using XOR operation

$\mathbf{u}_B = \mathbf{u}_{R,A} \oplus \mathbf{u}_A$ . Similarly, source node B can obtain the needed information by $\mathbf{u}_A = \mathbf{u}_{R,B} \oplus \mathbf{u}_B$; $\mathbf{u}_{R,B}$ is estimated based on $\mathbf{y}_B$.

This paper focuses on the MA phase. In the rest of this part, we mainly discuss it based on BPSK–QPSK.

## 3. Scheme designed for A-TWRC system

In this section, an encoding approach is designed to correlate the codewords from the source nodes to make a common non-binary linear decoder suitable for decoding at the relay node. Furthermore, the capability of the non-binary decoder at the relay node is verified by proving that the superposition of codewords from the source nodes is only the output of a virtual encoder, which inputs the superposition of the corresponding uncoded messages.

### 3.1 Encoders at the source nodes

For an asymmetric two-way channel system, different order modulations are applied to source nodes A and B. Therefore, at each source node, a channel encoder with a filed order is equal to that of the modulation of this source node.

In a symmetric situation, two source nodes can adopt the same linear code. That is, no modifications at the source nodes are needed. The decoder at the relay node simply selects the tanner graph corresponding to the encoders at the source nodes. Special belief propagation [21] is then designed according to the constraints at the variable nodes. However, in an asymmetric situation, modifications should be introduced into the source nodes as follows.

**Table 1.** Partial multiplication table

(a) GF(2)

| • | 0 | 1 |
|---|---|---|
| 0 | 0 | 0 |
| 1 | 0 | 1 |

(b) GF(4)

| • | 0 | 1 | … |
|---|---|---|---|
| 0 | 0 | 0 | … |
| 1 | 0 | 1 | … |
| X | 0 | X | … |
| X+1 | 0 | X+1 | … |

(c) GF(8)

| • | 0 | 1 | … |
|---|---|---|---|
| 0 | 0 | 0 | … |
| 1 | 0 | 1 | … |
| X | 0 | X | … |
| X+1 | 0 | X+1 | … |
| $X^2$ | 0 | $X^2$ | … |
| $X^2$+1 | 0 | $X^2$+1 | … |
| $X^2$+X | 0 | $X^2$+X | … |
| $X^2$+X+1 | 0 | $X^2$+X+1 | … |

Let $\mathbf{u}_A \in GF(4)$ and $\mathbf{u}_B \in GF(2)$ denote the uncoded words of length $K$ of A and B, respectively. $\mathbf{G}_4 \in GF(4)$ and $\mathbf{G}_2 \in GF(2)$ denote the generator matrixes adopted by A and B, respectively. To introduce the correlation between codewords from two source nodes, the generator matrixes are constructed by performing a Gaussian elimination on the same $\mathbf{H} \in GF(2)$ over $GF(4)$ and $GF(2)$, respectively, as $GF(4)$ is the extension field of $GF(2)$. Partial multiplication tables for $GF(q), q = 2,4,8$ are presented in **Table 1.** The elements of the Galois field illustrate a polynomial expression involving primitive elements X, which show two special polynomials 0 and 1. The table indicates that the multiplication for $GF(2)$ is included by that for $GF(4)$. Therefore, $\mathbf{G}_4$ is identical to $\mathbf{G}_2$ if they are

constructed by performing a Gaussian elimination on the same $\mathbf{H} \in GF(2)$. The same conclusion can be drawn for $\mathbf{G}_8 \in GF(8)$. The codewords of length $N$ of A and B are denoted by $\mathbf{c}_A = \mathbf{u}_A \cdot \mathbf{G}_4 \in GF(4)$ and $\mathbf{c}_B = \mathbf{u}_B \cdot \mathbf{G}_2 \in GF(2)$, respectively.

Afterwards, $\mathbf{c}_A$ are QPSK-modulated to $\mathbf{s}_A = \mathcal{M}_{\text{QPSK}}\{\mathbf{c}_A\}$, and $\mathbf{c}_B$ are BPSK-modulated to $\mathbf{s}_B = \mathcal{M}_{\text{BPSK}}\{\mathbf{c}_B\}$ according to the mapping rule $\{00,10,01,11\} \to \{1, j, -1, -j\}$ and $\{0,1\} \to \{1,-1\}$, respectively. For analytical convenience, the QPSK mapping rule may interchangeably be represented by the equivalent $\{00,10,01,11\} \to \{\sqrt{2}/2 + \sqrt{2}/2\, j, \sqrt{2}/2 - \sqrt{2}/2\, j, -\sqrt{2}/2 + \sqrt{2}/2\, j, -\sqrt{2}/2 - \sqrt{2}/2\, j\}$.

For the BPSK signal, let $\alpha_{\text{bpsk}} \in (\pm 1), \beta_{\text{bpsk}} = 0$ denote the alphabets of its real and imaginary components. For the QPSK signal, we have $\alpha_{\text{bpsk}}, \beta_{\text{bpsk}} \in (\pm 1)$, and their normalizing factor $\gamma_{\text{bpsk}} = 1, \gamma_{\text{qpsk}} = 2$. Let $\Re, \Im$ be the real and imaginary components of the superposing signal. Without noise, they can be expressed as

$$\begin{cases} \Re_{\text{sup}} = \left( \sqrt{\dfrac{E_{\text{bpsk}}}{\gamma_{\text{bpsk}}}} \alpha_{\text{bpsk}} + \sqrt{\dfrac{E_{\text{qpsk}}}{\gamma_{\text{qpsk}}}} \alpha_{\text{qpsk}} \right) \\ \Im_{\text{sup}} = \left( \sqrt{\dfrac{E_{\text{bpsk}}}{\gamma_{\text{bpsk}}}} \beta_{\text{bpsk}} + \sqrt{\dfrac{E_{\text{qpsk}}}{\gamma_{\text{qpsk}}}} \beta_{\text{qpsk}} \right) \end{cases} \tag{3}$$

where $E_{\text{bpsk}}$ and $E_{\text{qpsk}}$ are the average transmitting powers, and the power constraint $E_{\text{bpsk}} + E_{\text{qpsk}} = E_{\text{limit}}$ is assumed.

**Table 2.** Mapping rules for code bit $(c_A, c_B)$ and transmit signals $(s_A, s_B)$

| $i$ | $c_A$ | $c_B$ | $c_{A\oplus B}$ | $c_{AB}$ | $s_A$ | $s_B$ | $s_{A+B}$ |
|---|---|---|---|---|---|---|---|
| 0 | 0 | 0 | 0 | 0 | 1 | 1 | $h_A + h_B$ |
| 1 | 1 | 0 | 1 | 1 | -1 | 1 | $-h_A + h_B$ |
| 2 | X | 0 | X | X | j | 1 | $jh_A + h_B$ |
| 3 | X+1 | 0 | X+1 | X+1 | -j | 1 | $-jh_A + h_B$ |
| 4 | 0 | 1 | 1 | $X^2$ | 1 | -1 | $h_A - h_B$ |
| 5 | 1 | 1 | 0 | $X^2$+1 | -1 | -1 | $-h_A - h_B$ |
| 6 | X | 1 | X+1 | $X^2$+X | j | -1 | $jh_A - h_B$ |
| 7 | X+1 | 1 | X | $X^2$+X+1 | -j | -1 | $-jh_A - h_B$ |

The codeword $\mathbf{c}_A = [c_A(1), \ldots, c_A(N)]$ of source node A is composed of $N$ symbols $c_A(n)$. For notational simplicity and without loss of generality, the time index $n$ is omitted whenever possible. **Table 2** lists the basic relationships between the modulated signals $s_A$ and $s_B$ and the corresponding occurring code symbols $c_A$ and $c_B$. For the sake of subsequent

derivations and description, the XOR $c_{A\oplus B}=c_A\oplus c_B$ and $s_{A+B}\in\mathcal{S}_{AB}$ that present the noise-free signal levels at the relay node with

$$\mathcal{S}_{AB}=\{h_A+h_B,-h_A+h_B,jh_A+h_B,-jh_A+h_B,h_A-h_B,-h_A-h_B,jh_A-h_B,-jh_A-h_B\} \quad (4)$$

are also included. Moreover, the 8-ary symbol $c_{AB}=c_A+c_B\mathrm{X}^2$ is defined as an abbreviated symbolic notation for the eight different combinations of $c_A$ and $c_B$, i.e., $c_{AB}\in\mathcal{C}_{AB}$ with the Galois field

$$\mathcal{C}_{AB}=\{0,1,\mathrm{X},\mathrm{X}+1,\mathrm{X}^2,\mathrm{X}^2+1,\mathrm{X}^2+\mathrm{X},\mathrm{X}^2+\mathrm{X}+1\} \quad (5)$$

where $c_{AB}=\mathcal{C}_{AB}(i)$ and $s_{A+B}=\mathcal{S}_{AB}(i)$ denote the $i$-th event $(0\le i\le 7)$ in $GF(8)$ and in the received signal space, respectively.

### 3.2 Decoder at the relay node

The relay node first decodes the superposition of $c_A$ and $c_B$ from the superposition signals to obtain the superposition of $u_A$ and $u_B$, specifically to generate $u_{AB}$ from $c_{AB}$ in this paper. The overall effectiveness of the encoders at the source nodes can be treated as a virtual encoder, which inputs $u_{AB}$ and outputs $c_{AB}$ as shown in **Fig. 2**. Subsequently, we prove that the virtual encoder is as simple as a common linear encoder over $GF(8)$ following the aforementioned approach of encoding at the source nodes. This approach makes the common non-binary decoder over $GF(8)$ capable without modifying the tanner graph nor decoding algorithm.

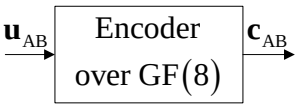


**Fig. 2.** Virtual encoder over GF(8)

For an A-TWRC, if $\mathbf{c}_A$ is a codeword of $\Gamma$ over $GF(4)$ and $\mathbf{c}_B$ is codeword of the same linear channel code over $GF(2)$, then $\mathbf{c}_{AB}$ is only a valid codeword of the linear virtual channel code $\Gamma$ over $GF(8)$ after the following combination:

$$c_{AB}(n)=c_A(n)+c_B(n)\mathrm{X}^2. \quad (6)$$

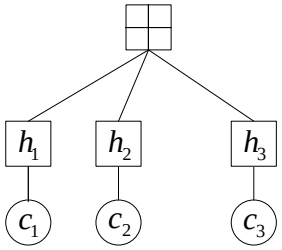


**Fig. 3.** A check node with degree 3

Without loss of generality, a check node with degree 3 is assumed as shown in **Fig. 3**, where $h_1, h_2, h_3$ are the non-zero entries in the same row of the parity check matrix H and $c_{i1}, c_{i2}, c_{i3}$ are the variable nodes (circular blocks at the bottom) that participate in the check node (square block at the top) from source $i, i \in \{\mathrm{A}, \mathrm{B}\}$. The known conditions are given as follows:

$$\begin{cases} c_{\mathrm{A1}} \cdot h_1 + c_{\mathrm{A2}} \cdot h_2 = c_{\mathrm{A3}} \cdot h_3 & \text{over } GF(4) \\ c_{\mathrm{B1}} \cdot h_1 + c_{\mathrm{B2}} \cdot h_2 = c_{\mathrm{B3}} \cdot h_3 & \text{over } GF(2). \\ h_1 = h_2 = h_3 = 1 \end{cases} \tag{7}$$

The following equation should hold:

$$\left(c_{\mathrm{A1}} + c_{\mathrm{B1}} \cdot \mathrm{X}^2\right) \cdot h_1 + \left(c_{\mathrm{A2}} + c_{\mathrm{B2}} \cdot \mathrm{X}^2\right) \cdot h_2 = \left(c_{\mathrm{A3}} + c_{\mathrm{B3}} \cdot \mathrm{X}^2\right) \cdot h_3. \tag{8}$$

For this purpose, all the elements are illustrated as polynomial expressions:

$$c_{\mathrm{A1}} = \left(a_1 \mathrm{X} + b_1\right), c_{\mathrm{A2}} = \left(c_1 \mathrm{X} + d_1\right), c_{\mathrm{A3}} = \left(e_1 \mathrm{X} + f_1\right), c_{\mathrm{B1}} = b_2, c_{\mathrm{B2}} = d_2, c_{\mathrm{B3}} = f_2. \tag{9}$$

Then,

$$\begin{aligned} \left(c_{\mathrm{A1}} + c_{\mathrm{B1}} \cdot \mathrm{X}^2\right) \cdot h_1 + \left(c_{\mathrm{A2}} + c_{\mathrm{B2}} \cdot \mathrm{X}^2\right) \cdot h_2 &= \left(a_1 \mathrm{X} + b_1 + b_2 \cdot \mathrm{X}^2\right) + \left(c_1 \mathrm{X} + d_1 + d_2 \cdot \mathrm{X}^2\right) \\ &= \left[\left(a_1 \mathrm{X} + b_1\right) + \left(c_1 \mathrm{X} + \mathrm{d}_1\right)\right] + \left[b_2 + d_2\right] \cdot \mathrm{X}^2 \\ &= \left[\left(e_1 \mathrm{X} + f_1\right)\right] + \left[f_2\right] \cdot \mathrm{X}^2 \\ &= \left(c_{\mathrm{A3}} + c_{\mathrm{B3}} \cdot \mathrm{X}^2\right) \cdot h_3 \end{aligned} \tag{10}$$

Thus, an FFT-SPA [22] for $GF(8)$ can be used for decoding.

Suppose the eight symbol signals $c_{\mathrm{AB}}$ and $s_{\mathrm{A+B}}$ are equally likely. Then the *a priori* probabilities for $c_{\mathrm{AB}} = \mathcal{C}_{\mathrm{AB}}(i)$ and $s_{\mathrm{A+B}} = \mathcal{S}_{\mathrm{AB}}(i)$ are given by

$$\Pr\left\{c_{\mathrm{AB}} = \mathcal{C}_{\mathrm{AB}}(i)\right\} = p\left\{s_{\mathrm{A+B}} = \mathcal{S}_{\mathrm{AB}}(i)\right\} = \frac{1}{8}. \tag{11}$$

The conditional probability density for a given signal $s_{\mathrm{A+B}} \in \mathcal{S}_{\mathrm{AB}}$ is calculated as

$$p\left\{y_{\mathrm{R}} \middle| s_{\mathrm{A+B}} = \mathcal{S}_{\mathrm{AB}}(i)\right\} = \frac{1}{2\pi\sigma^2} \exp\left(-\frac{\left(y_{\mathrm{R}} - \mathcal{S}_{\mathrm{AB}}(i)\right)^2}{2\sigma^2}\right). \tag{12}$$

Thus, the probability that the signal $s_{\mathrm{A+B}} = \mathcal{S}_{\mathrm{AB}}(i)$ is transmitted given the received signal $y_{\mathrm{R}}$ is

$$\begin{aligned} P_i &= \Pr\left(c_{\mathrm{AB}} = \mathcal{C}_{\mathrm{AB}}(i) \middle| y_{\mathrm{R}}\right) = p\left\{s_{\mathrm{A+B}} = \mathcal{S}_{\mathrm{AB}}(i) \middle| y_{\mathrm{R}}\right\} \\ &= p\left\{y_{\mathrm{R}} \middle| s_{\mathrm{A+B}} = \mathcal{S}_{\mathrm{AB}}(i)\right\} \frac{\Pr\left(s_{\mathrm{A+B}} = \mathcal{S}_{\mathrm{AB}}(i)\right)}{\Pr\left(y_{\mathrm{R}}\right)} \\ &= p\left\{y_{\mathrm{R}} \middle| s_{\mathrm{A+B}} = \mathcal{S}_{\mathrm{AB}}(i)\right\} \frac{1}{\xi} \end{aligned} \tag{13}$$

As $\sum P_i = 1$ , the constant $\xi = 8\Pr\left(y_{\mathrm{R}}\right)$ in (13) can be calculated and is used as a normalization factor. Thus the *a posteriori* probabilities (APPs) vector that equals

$$\mathbf{P} = \left[P_0\ P_1\ P_2\ P_3\ P_4\ P_5\ P_6\ P_7\right] \tag{14}$$

is fed to the decoder as an initial message of one variable [22].

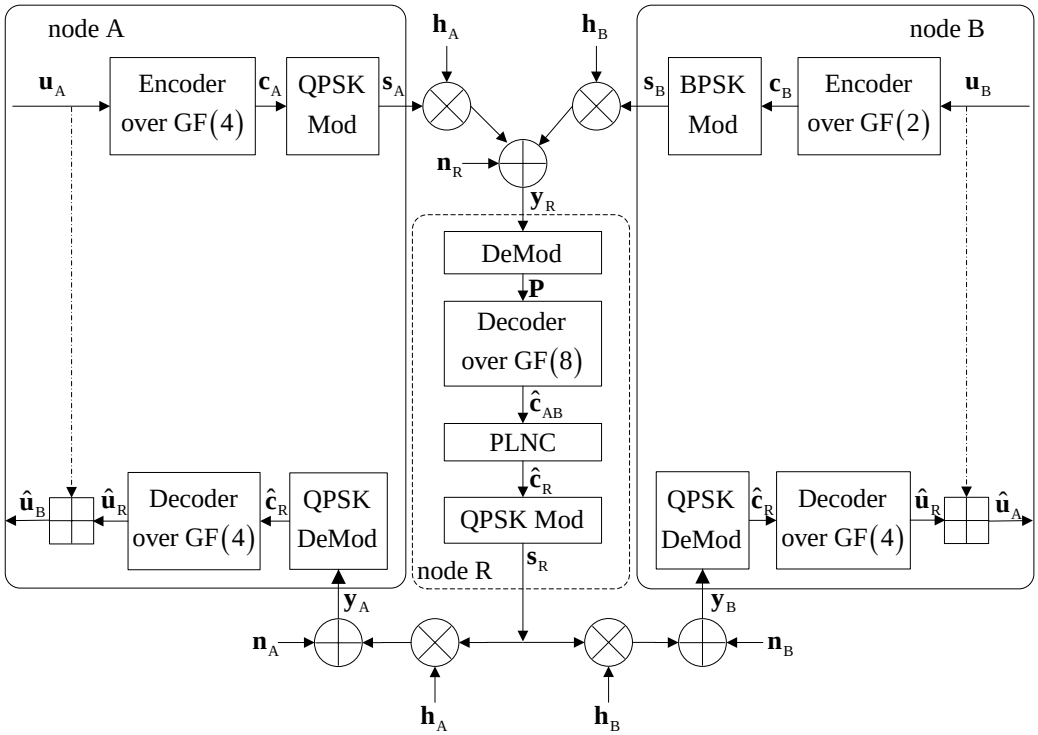


**Fig. 4.** Overall diagram of the designed scheme

The decoding $y_{\mathrm{R}} \to \hat{c}_{\mathrm{AB}}$ with respect to $GF(8)$ is executed and then the PLNC $\hat{c}_{\mathrm{AB}} \to c_{\mathrm{R}}$ by a corresponding mapping rule is performed according to **Table 2**. Specifically, the following combined APP vector

$$\begin{aligned} &\left[\Pr\left\{c_{\mathrm{A}\oplus\mathrm{B}} = 0 \middle| y_{\mathrm{R}}\right\} \Pr\left\{c_{\mathrm{A}\oplus\mathrm{B}} = 1 \middle| y_{\mathrm{R}}\right\} \Pr\left\{c_{\mathrm{A}\oplus\mathrm{B}} = \mathrm{X} \middle| y_{\mathrm{R}}\right\} \Pr\left\{c_{\mathrm{A}\oplus\mathrm{B}} = \mathrm{X}+1 \middle| y_{\mathrm{R}}\right\}\right] \\ &\qquad = \left[P_0 + P_5\ P_1 + P_4\ P_2 + P_7\ P_3 + P_6\right] \end{aligned} \tag{15}$$

is obtained after PLNC mapping. Then, the broadcasts $\mathbf{s}_{\mathrm{R}} = \mathcal{M}_{\mathrm{QPSK}}\{\hat{\mathbf{c}}_{\mathrm{R}}\}$ are relayed to both source nodes following hard-deciding the combined APP vector to obtain $\hat{\mathbf{c}}_{\mathrm{R}}$.

### 3.3 Decoders at the sources nodes

Common decoders are used at the source nodes although note that both nodes adopt the same decoder over $GF(4)$. That is, the orders of encoder and decoder of node B are different. As previously mentioned, identical generator matrixes are used by source nodes A and B, and $\mathbf{c}_{\mathrm{B}}$ is considered a valid codeword generated by $\mathbf{G}_4$ over $GF(4)$. Then, the source nodes can derive wanted messages from the other node by a modulo-4 summing output of the decoder with self-information. **Fig. 4** illustrates the overall diagram of the designed scheme.

## 4. Simulation Results and Analysis

The authors of [15] argue that greater signal power does not result in better performance for an A-TWRC with PLNC. The performance of an A-TWRC is related not only to the total power but also to the power matching ratio of the two transmitters. In this section, numerical results are provided to evaluate the designed scheme and effect of the power matching ratio $\lambda$ under different numbers of iteration and codeword lengths and to find the optimum power matching ratio $\lambda_{op}$. Then, the performances of the designed scheme under different SNRs are compared. The performance under an imperfect channel estimation is also evaluated.

In the simulations, the perfect synchronization of all nodes is assumed, and optimized LDPC codes from [23] with code rate $R_c = 1/2$ are applied. The SNR defined in [15] as $\mathrm{SNR}=\left(E_{QPSK}+E_{BPSK}\right)/N_0$ is used. To consider the optimum ratio in the fading channel, fading coefficients are considered through a relative deviation described in [11], where the fading coefficient for A is always $h_{\mathrm{A}}=1$ and the coefficient for B is a normal distribution around the unit circle, i.e., $\left|\alpha^{\theta}\right|=1$ with $\theta \sim U(-\pi,\pi)$. In the imperfect channel estimation, the channel estimations with errors are modeled as $h_i = \hat{h}_i + e_h, i \in \{A,B\}$, where $\hat{h}_i$ is the channel estimated coefficient and $e_h$ is the channel estimated error, which is a complex Gaussian with zero mean and variance $\sigma_{e_h}^2$.

**Fig. 5** presents the bit error rate (BER) performance of the different code lengths (96, 204, 408, 816, 2640 and 4000) when the iteration numbers are set to 5 and $SNR = 6$. The code lengths are selected to cover the range from short length (a few hundred bits) [24] to moderate length (103<N<104 bits) [25]. All the curves go down first then rise because of the increase in $\lambda$. In general, a larger code length leads to a smaller BER in a point-to-point scenario. However, an inappropriate matching ratio can eliminate the improvement caused by the larger code length. None of the improvement is given by the larger code length when $\lambda < 0.5$ or $\lambda > 4$. Aside from the first two curves (96, 204), all other curves with different code lengths have the same optimum power ratio $\lambda_{op} = 2.1$. The reason is that the BP decoding introduces observable performance loss when dealing with the LDPC codes of lengths between a hundred and a few thousand bits [24]. As a decoder over GF(8) is used at the relay node, it is equal to 768 bits ($96\times 8$) or 1632 bits ($204\times 8$) when an LDPC with length of 96 or 204 is used at the source nodes, respectively.

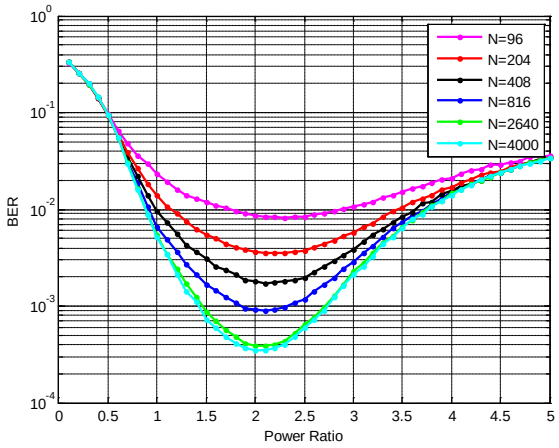


**Fig. 5.** BER performance for different code lengths

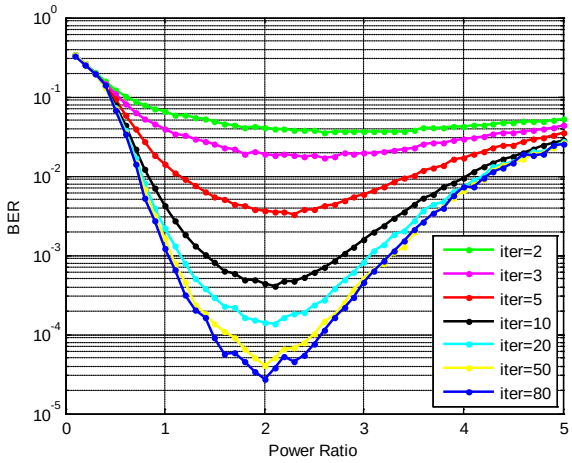


**Fig. 6.** BER performance under different iteration numbers

**Fig. 6** illustrates the BER performance under identical code lengths $N = 202$ and $SNR = 6$ but with different iteration numbers set to 2, 3, 5, 10, 20, 50, and 80. Unlike code length, which has no effect on $\lambda_{op}$, iteration number can change $\lambda_{op}$. The optimum ratio point decreases with the increase in iteration number. For instance, the optimum ratio point is about 2.5 when iterating 3 times, and it decreases to 2.0 when number of iteration is 50. Futhermore, the decrease rate also goes down gradually with the increase in iteration number, and $\lambda_{op}$ converges to 2.0 when the numbers of iteration are large enough. Intuitively, this action is reasonable as, without noise, $\lambda_{op}$=2.0 makes the superposition signals similar to an 8QAM-like constellation. Similarly, the improvement caused by larger numbers of iteration is counterbalanced by the inappropriate matching ratio when $\lambda < 0.5$ or $\lambda > 5$.

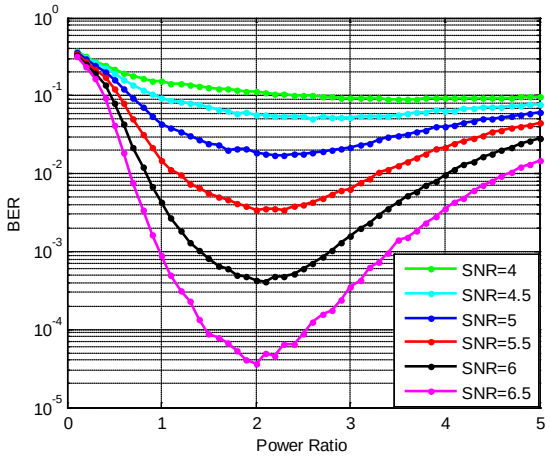


**Fig. 7.** Performance curves with $SNR = 4$ to 6.5

**Fig. 7** presents the performance curves when $SNR = 4 - 6.5$ to determine the effect of different SNRs. The curves in **Fig. 7** have a similar pattern to those in **Fig. 6, where** $\lambda_{op}$ converges to 2.0 when the SNRs are large enough.

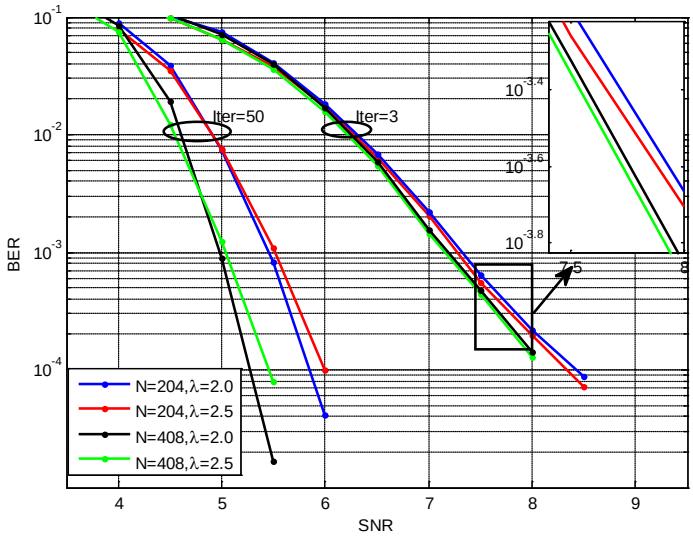


**Fig. 8.** Overall influence of power ratio

The overall effect of the power ratio is also illustrated in **Fig. 8**. The performance with $\lambda = 2.0$ is better than that with $\lambda = 2.5$ when the iteration numbers are set to 50. By contrast, $\lambda = 2.5$ leads to a better performance when iterating 3 times. At the same time, the effect of SNR is aslo reflexed in **Fig. 8**. A better error performance is achieved when SNR is lower, e.g., $SNR < 4.6$. The curve with $\lambda = 2.5$ outperforms that with $\lambda = 2.0$ although they have 50 times of iteration. Therefore, SNR is a predominant factor that mostly affects $\lambda_{op}$.

**Fig. 9** presents the effect of the channel estimation error on system performance. The code length is set to $N = 204$, and the iteration number is 50. The channel error power $\sigma_e^2 = 0.01$ and 0.1 are selected to evaluate the effect of the channel estimation error. As in the case of a

perfect channel estimation, all the curves are also concave with an optimum ratio. However, $\lambda_{op}$ deviates to a larger ratio when error power is larger. When $\sigma_e^2 = 0.01$, the optimum ratio $\lambda_{op} = 2.1$ deviates from 2.0 in a perfect CSI situation. The ratio deviates to a much larger $\lambda_{op} = 2.3$ when $\sigma_e^2 = 0.1$.

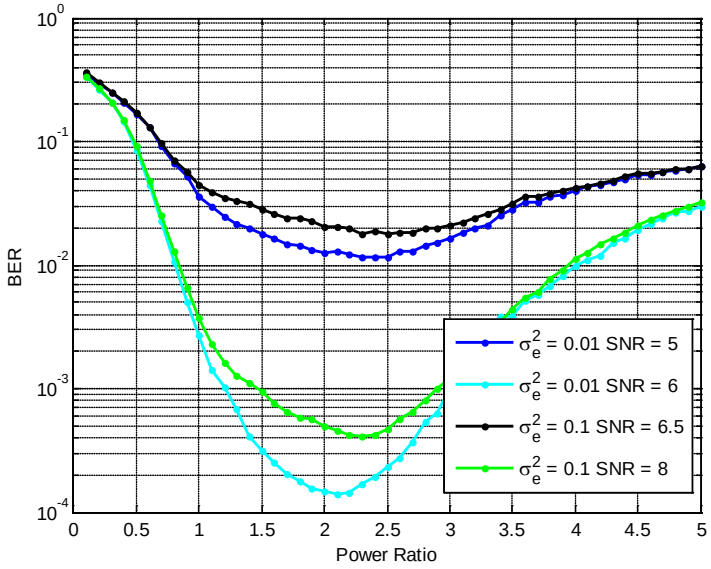


**Fig. 9.** BER performance under imperfect channel estimation information

## 5. Conclusion

This study designed a G-JCNC scheme in an A-TWRC scenario. A new designed encoder that is used by both source nodes and that can correlate the codewords with different orders is presented. This encoder makes the decoder at the relay node as simple as a common non-binary decoder. The capability of the non-binary decoder at the relay node is verified. Based on the comparisons of the simulation results, an inappropriate matching ratio can eliminate the improvement caused by a larger code length and larger numbers of iteration. The moderate or the larger code length has no effect on the optimum power matching, but both the numbers of iteration and SNR have and effect. Moreover, SNR is a more predominant factor than iteration number. The optimum power matching converges to 2.0 when the numbers of iteration or SNRs are large enough. In an imperfect channel esitmation, all the curves are also concave with an optimum ratio. However, the optimum ratio deviates to a larger one when the estimation error power is larger.

## References

[1] Y. Zou, B. Champagne, W. P. Zhu and L. Hanzo, "Relay-selection improves the security-reliability trade-off in cognitive radio systems," *IEEE Trans. Communications*, vol. 63, no. 1, pp. 215-228, January, 2015. Article (CrossRef Link)

[2] Y. Zou, X. Wang, W. Shen and L. Hanzo, "Security versus reliability analysis of opportunistic relaying," *IEEE Trans. Vehicular Technology*, vol. 63, no. 6, pp. 2653-2661, July, 2014. Article (CrossRef Link)

[3] Y. Zou, J. Zhu and B. Zheng, "A fully distributed opportunistic network coding scheme for cellular relay networks," in *Proc. of Wireless Communications and Networking Conference (WCNC)*, pp. 2937-2942, April 7-10, 2013. Article (CrossRef Link)
[4] S. C. Liew, S. Zhang and L. Lu, "Physical-layer network coding: Tutorial, survey, and beyond," *Physical Communication*, vol. 6, pp. 4-42, March, 2013. Article (CrossRef Link)
[5] R. H. Louie, Y. Li and B. Vucetic, "Practical physical layer network coding for two-way relay channels: performance analysis and comparison," *IEEE Trans. Wireless Commun.*, vol. 9, no. 2, pp. 764-777, February, 2010. Article (CrossRef Link)
[6] S. Zhang, S. C. Liew and P. P. Lam, "Hot topic: physical-layer network coding," in *Proc. of 12th Int. Conf. on Mobile Computing and Networking*, pp. 358-365, September 29, 2006. Article (CrossRef Link)
[7] A. Zhan and C. He, , "Joint design of channel coding and physical network coding for wireless networks," in *Proc. of Int. Conf. on Neural Networks and Signal Processing*, pp. 512-516, June 7-11, 2008. Article (CrossRef Link)
[8] S. Zhang and S. C. Liew, "Channel coding and decoding in a relay system operated with physical-layer network coding," *IEEE Journal on Selected Areas in Communications*, pp.250-257, vol. 27, no. 5, pp. 788-796, June, 2009. Article (CrossRef Link)
[9] Y. Lang, D. Wübben and K. D. Kammeyer, "An improved physical layer network coding scheme for two-way relay systems," in *Proc. of ITG Workshop on Smart Antennas (WSA)*, pp. 512-516, February 23-24, 2010. Article (CrossRef Link)
[10] D. Wubben and Y. Lang, "Generalized joint channel coding and physical network coding for two-way relay systems," in *Proc. of IEEE 71st Vehicular Technology Conference*, pp. 1-5, May 16-19, 2010. Article (CrossRef Link)
[11] D. Wübben and Y. Lang, "Generalized sum-product algorithm for joint channel decoding and physical-layer network coding in two-way relay systems," in *Proc. of IEEE Global Telecommunications Conference*, pp. 1-5, December 6-10, 2010. Article (CrossRef Link)
[12] D. Wübben, "Joint channel decoding and physical-layer network coding in two-way QPSK relay systems by a generalized Sum-Product Algorithm," in *Proc. of 7th IEEE Int. Symposium on Wireless Communication Systems (ISWCS)*, pp. 576-580, September 19-22, 2010. Article (CrossRef Link)
[13] H. Wei, B. Zheng and X. Ji, "A novel design of physical layer network coding in strong asymmetric two-way relay channels," *EURASIP Journal on Wireless Communications and Networking*, vol. 2013, no. 1, pp. 1-10, February, 2013. Article (CrossRef Link)
[14] L. Wang and Z. Wu, "BER analysis of physical layer network coding with PSK modulations for two-way relay channels," in *Proc. of IEEE Int. Conf. on Signal Processing, Communication and Computing (ICSPCC)*, pp. 484-489, August 12-15, 2012. Article (CrossRef Link)
[15] X. Zhang, Y. Li, J. Lin, L. Guo and Z. He, "On performance of judging region and power allocation for wireless network coding with asymmetric modulation," in *Proc. of IEEE Vehicular Technology Conference (VTC Fall)*, pp. 1-5, September 5-8, 2011. Article (CrossRef Link)
[16] X. Zhang, Y. Li, J. Lin, J. Di and R. Han, "Asymmetric network coding in two-way relay channels for cooperative communications: SER performance and power matching," in *Proc. of 14th Int. Symposium on Wireless Personal Multimedia Communications (WPMC)*, pp.1-5, October 3-7, 2011.
[17] L. Bo, W. Gang, P. H. J. Chong, Y. Hongjuan, Y. Guan and S. Xuejun, "Performance of physical-layer network coding in asymmetric two-way relay channels," *China Communications*, vol. 10, no. 10, pp. 65-73, October, 2013. Article (CrossRef Link)
[18] B. Li, G. Wang, H. Yang, P. H. J. Chong and Y. Guan, "Combined orthogonal physical-layer network coding (COPNC) for asymmetric two-way relay channels," in *Proc. of 9th Int. Conf. on Information, Communications and Signal Processing (ICICS)*, pp. 1-4, December 10-13, 2013. Article (CrossRef Link)
[19] B. Li, G. Wang, H. Yang and R. Liu, "Performance of physical-layer network coding in asymmetric rayleigh fading two-way relay communication systems," *Information Technology Journal*, vol. 12, no. 9, pp. 1804-1810, 2013. Article (CrossRef Link)

[20] S. C. Liew, L. Lu and S. Zhang, "A Primer on Physical-Layer Network Coding," *Morgan & Claypool*, 2015. Article (CrossRef Link)
[21] J. G. Proakis and M. Salehi, "Digital communications 5th Edition," *McGraw-Hill*, 2007.
[22] A. Voicila, D. Declercq, F. Verdier, M. Fossorier and P. Urard, "Low-complexity decoding for non-binary LDPC codes in high order fields," *IEEE Trans. Communications*, vol. 58, no. 5, pp. 1365-1375, May, 2010. Article (CrossRef Link)
[23] D. MacKay and E. C. Codes, "David MacKay's Gallager code resources," *Dostupný z URL:< http://www. inference. phy. cam. ac. uk/mackay/CodesFiles. html* (2009).
[24] E. Cavus and B. Daneshrad, "A performance improvement and error floor avoidance technique for belief propagation decoding of LDPC codes," in *Proc. of IEEE 16th Int. Symposium on Personal, Indoor and Mobile Radio Communications*, pp. 2386-2390, September 11-14, 2005. Article (CrossRef Link)
[25] M. Yang, W. E. Ryan and Y. Li, "Design of efficiently encodable moderate-length high-rate irregular LDPC codes," *IEEE Trans. Communications*, vol. 52, no. 4, pp. 564-571, April, 2004. Article (CrossRef Link)

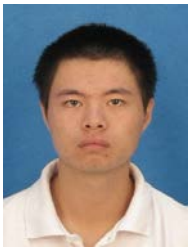

**Shengqiang Shen** received the B.S. degree in Information Engineering from China University of Mining and Technology, Xuzhou, P.R. China, in 2013, and now he is a Ph.D. Candidate in Information and Communication Engineering of China University of Mining and Technology, Xuzhou, P.R. China. Since 2013, his main research interests are wireless communications, joint network and channel coding and indoor localization.

**Shiyin Li** was born in 1971. He received his Ph.D. degree in Information and Communication Engineering of China University of Mining and Technology, Xuzhou, P.R. China., in 2010. Since 2010 he has been a Professor in School of Information and Electrical Engineering, China University of Mining and Technology. He is the Head of the Department of Information Engineering. His main research interests are wireless communication and network congestion control.

**Zongyan Li** received her Ph.D. degree in communications and information system from Beijing University of Posts and Telecommunications, China, in 2012. She is a lecture in China University of Mining and Technology. Her current research interests are in iterative decoding algorithms, network coding, and cooperative communications.